Discovery of Novel 1,2,3-Triazole Analogues as Anti-Tuberculosis agents Using 3D QSAR, Molecular Docking, and In Silico ADMET Screening

Adib Ghaleb[a],*, Adnane Aouidate[a], Mohammed Bouachrine[b], Tahar Lakhlifi[a] and Abdelouahid Sbai[a]

[a]Faculty of Science, Moulay Ismail University, Meknes, Morocco
[b]EST, Moulay Ismail University, Meknes, Morocco
(Received 1 October 2018 Accepted 15 December 2018)

Heterocyclic moieties have become more interesting for chemists, pharmacologists, microbiologists, and other researchers owing to their indomitable biological potential as anti-infective agents. Among heterocyclic compounds, 1,2,3-triazole nucleus is one of the most important and well-known heterocycles. Triazole core is considered as essential structure in medicinal chemistry which is widely used to synthesize molecules with medical benefits. In this work, a set of triazole analogues were identified as anti-tubercular agents through a series of computer-aided drug design processes, including three-dimensional quantitative structure-activity relationship (3D-QSAR) modeling, molecular docking, and ADMET studies to determine properties of these new proposed drugs. The CoMFA and CoMSIA models employed for a training set of 25 compounds reliable values of Q^2 (0.63 and 0.65, respectively) and R^2 (0.85 and 0.71, respectively). These results indicate that the developed models possess good predictive ability. Based on the 3D-QSAR contours, new molecules with high predicted activities were designed. Moreover, surflex-docking was applied to highlight the important interactions between the ligand and mycobacterium tuberculosis receptor, supporting the stability of the predicted molecules in the receptor. In silico ADMET results show good properties for these new anti-tubercular agents.

Keywords: 3D-QSAR, Surflex-docking, In silico ADMET, Anti-tubercular, Triazole

INTRODUCTION

Tuberculosis is a contagious disease with comparatively high mortality worldwide which is considered as the second cause of death from a single infectious agent [1]. The overall rate is increasing by 0.4% per year. It is estimated that one-third of world population is infected by tuberculosis, and 95% death occurs in developing countries [2]. The function of some available drugs used for the treatment of tuberculosis is based on their effective anti-tuberculosis activities, however, multidrug-resistant strains of Mycobacterium tuberculosis seriously threaten tuberculosis (TB) control and prevention efforts which demands the need for novel anti-tubercular agents with better activities.

In this regard, we developed a quantitative structure-activity relationship (QSAR) model to propose new effective potent drugs. QSAR methodology is an essential tool in modern medicinal chemistry. It attempts to relate the biological activity of a series of chemicals to their physicochemical and structural properties based on the hypothesis that similar structures have similar properties and that the more differences there are between molecules. The harder it is to correlate their physicochemical properties and biological activities, whereas such correlations between highly similar molecules are much easier [3]. The application of QSAR to molecular modeling and drug design has led to the inclusion of tools developed in the field of computational chemistry. They have been used to predict a large number of biological endpoints and shed light on the reaction mechanism, whether it is toxicological or pharmacological [4].

*Corresponding author. E-mail: adib.ghaleb@gmail.com

In this work, comparative molecular field analysis (CoMFA) [5] and comparative molecular similarity indices analysis (CoMSIA) [6] were carried out to predict the activity of 31 triazole compounds obtained from literature, present anti-tubercular activity [7], therefore suggest new competent drugs against MTB strains.

Surflex-Docking is used to determine the stability of the new proposed agents in mycobacterium tuberculosis receptor (PDB entry code: 5UH5), and study their interactions with the residues. Moreover, we performed an in silico study absorption, distribution, metabolism, excretion, and toxicity (ADMET) to determine the pharmacokinetic properties of the best proposed competent anti-tubercular drug.

MATERIALS AND METHODS

A database of 31 compounds consisting of 1,2,3-triazole derivatives as anti-tubercular agents was divided into two sets; 25 compounds were selected as training set and 6 compounds were selected as test set, based on a random selection to evaluate the ability of the model obtained. The structures and biological activities of both the training and test sets are given in Table 1. These data sets were used to construct 3D-QSAR (CoMFA and CoMSIA) models and to analyze their physicochemical properties. MIC activity was measured previously in $\mu g\ ml^{-1}$. We converted them to micromolar values ($\mu g\ ml^{-1}$) and finally recalculated to pMIC values as log(1/MIC). The pMIC values presented in Table 1 were used as the dependent variables in all subsequently developed PLS models.

Three-dimensional structure building (Fig. 1) and all optimizations were performed using the Sybyl 2.0 program package [8]. Discovery Studio Visualizer [9] and MOLCAD (Molecular Computer Aided Design) programs were used to visualize the interactions between molecules and receptor. ADMET properties were determined using Admetsar [10] and pKCSM predictors [11].

Minimization and Alignment

Molecular structures were sketched with sketch module in SYBYL and optimized using Tripos force field [12] with the Gasteiger-Huckel charges [13] by conjugated gradient method-with gradient convergence criteria of 0.01 $kcal\ mol^{-1}$. Simulated annealing on the optimized structures was performed with 20 cycles. Molecular alignment is one of the most sensitive parameters in 3D-QSAR analyses. In this work, all molecules were aligned on the common core, C(OC1=CC=CC=C1)C1=CN(N=N1)C1=CC=CC=C1, using the simple alignment method in Sybyl [14]. The most active compound 13 was used as template. The superimposed structures of aligned data set are shown in Fig. 2.
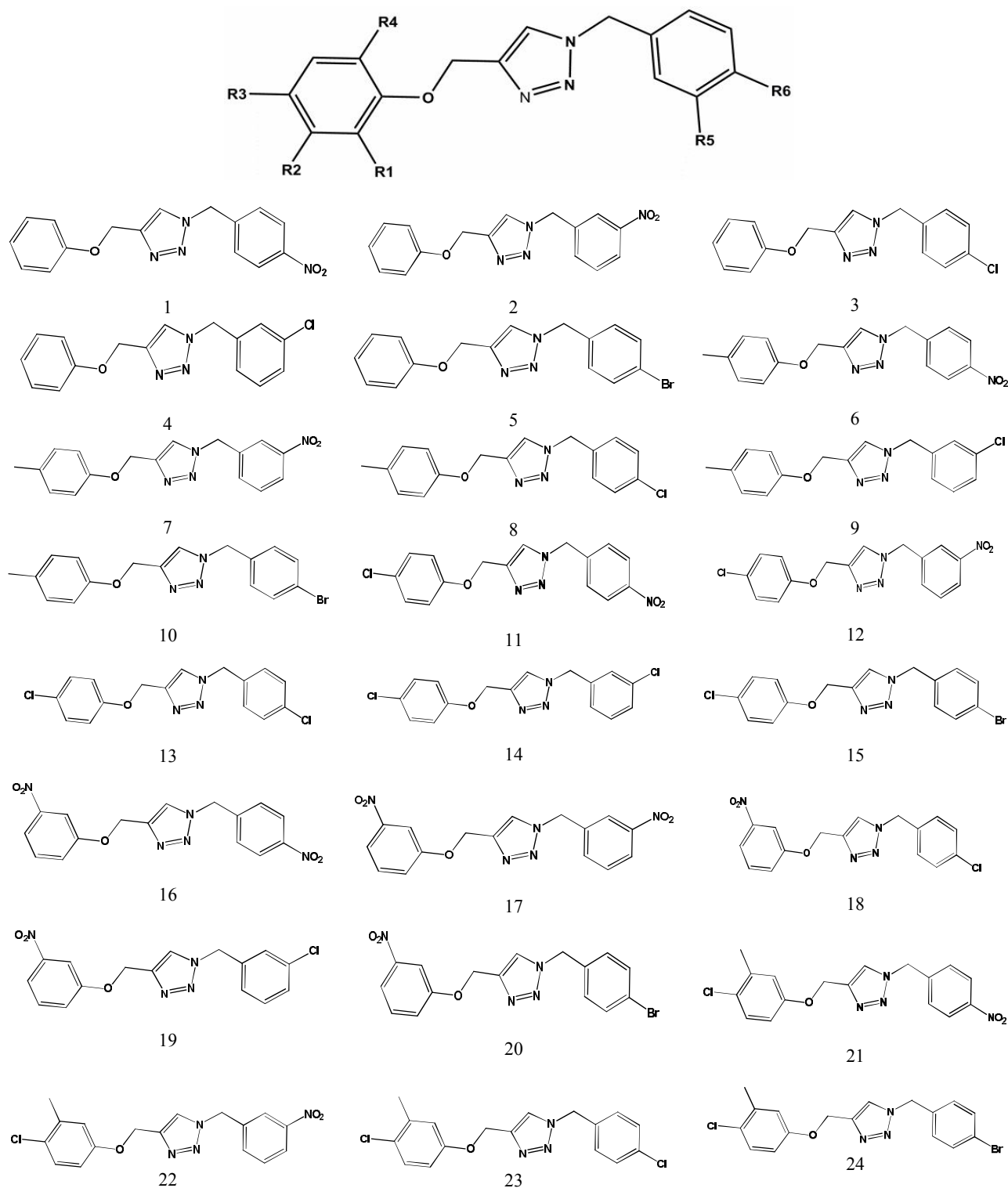
3D QSAR Studies

To understand and explore the contributions of electrostatic, steric and hydrophobic fields in different compounds of the data set and to create predictive 3D QSAR models, CoMFA and CoMSIA studies were performed based on the molecular alignment strategy, as previously described in the literature [15].

CoMFA and CoMSIA

Based on the molecular alignment, CoMFA and CoMSIA studies were performed to analyze the specific contributions of steric, electrostatic, and hydrophobic effects. The CoMFA method allows calculating steric and electrostatic properties according to the Lennard-Jones and Coulomb potentials, respectively. Using the CoMSIA approach, we calculated the similarity indices in the space surrounding each of the molecules in the dataset. CoMFA steric and electrostatic interaction fields were calculated at each lattice intersection point of a regularly spaced grid of 2.0 Å. The default value of 30 $kcal\ mol^{-1}$ was set as a maximum steric and electrostatic energy cutoff [16]. With standard options for scaling of variables, the regression analysis was carried out using the full cross-validated partial least squares (PLS) method (leave-one-out) [17]. The minimum sigma (column filtering) was set to 2.0 $kcal\ mol^{-1}$ to improve the signal-to-noise ratio by omitting the lattice points whose energy variation was below this threshold. The final non-cross-validated model was developed using optimal number of components that had both the highest Q^2 value and the smallest value of standard error predictions. The predictive r^2 was used to evaluate the predictive power of the CoMFA model and was based only on the test set. Several CoMFA models were built by considering

Table 1. Anti-tubercular and Predicted Activities of 1,2,3-Triazole Derivatives

No.	$_pMIC^a$	CoMFA		CoMSIA	
		Predicted	Residuals	Predicted	Residuals
1	4.55	4.499	0.051	4.573	-0.023
2	4.52	4.562	-0.042	4.625	-0.105
*3	4.52	4.519	0.001	4.511	0.009
4	4.55	4.577	-0.027	4.695	-0.145
5	4.54	4.559	-0.019	4.705	-0.165
*6	4.52	4.346	0.174	4.533	-0.013
7	4.52	4.536	-0.016	4.675	-0.155
8	4.61	4.553	0.057	4.722	-0.112
9	4.54	4.482	0.058	4.705	-0.165
10	4.52	4.476	0.044	4.720	-0.2
11	4.56	4.809	-0.249	4.721	-0.161
*12	4.53	4.718	-0.188	4.521	-0.009
13	5.08	5.002	0.078	4.754	0.326
*14	4.59	4.281	-0.691	4.562	0.028
15	5.23	5.096	0.134	4.757	0.473
16	4	4.070	-0.07	4.007	-0.007
*17	4.52	4.234	0.286	4.516	0.004
18	4	4.106	-0.106	4.036	-0.036
19	4	3.876	0.124	3.973	0.027
20	4	4.033	-0.033	4.009	-0.009
21	4.55	4.347	0.203	4.432	0.118
22	4.52	4.501	0.019	4.446	0.074
23	4.57	4.622	-0.052	4.499	0.071
24	4.52	4.708	-0.188	4.513	0.007
*25	4.52	4.721	-0.201	4.539	-0.019
26	4.52	4.600	-0.08	4.516	0.004
27	5.11	4.849	0.261	4.649	0.461
28	4.52	4.582	-0.062	4.594	-0.074
29	4.55	4.734	-0.184	4.637	-0.087
30	4.52	4.436	0.084	4.565	-0.045
31	4.52	4.503	0.017	4.593	-0.073

Fig. 1. Chemical structure of the studied compounds.

25

26

27

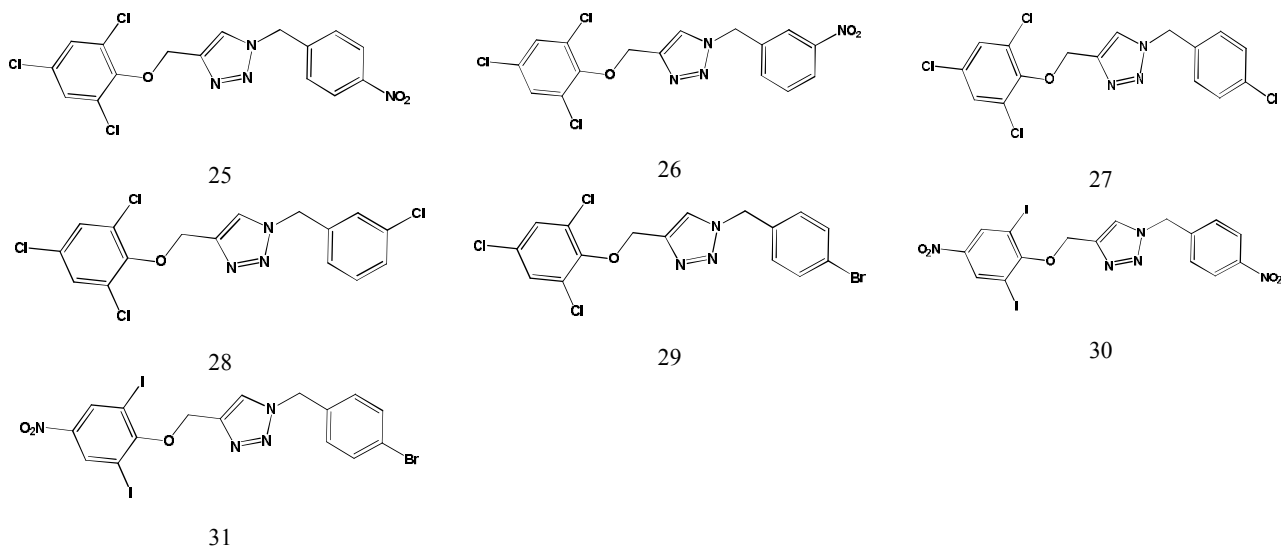28

29

30

31

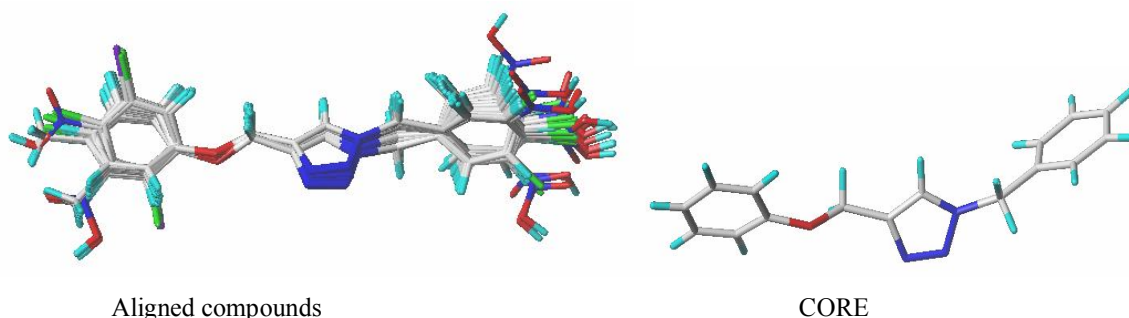**Fig. 1.** Continued.

Aligned compounds

CORE

Fig. 2. 3D-QSAR structure superposition and alignment of training set using molecule 13 as a template.

permutations of molecules between training and test sets. The best model amongst them was chosen, based on high Q^2, r^2 values and small Standard Error of Estimate (SEE) value. In CoMSIA, a distance-dependent Gaussian-type physicochemical property has been adopted to avoid singularities at the atomic positions and dramatic changes of potential energy for grids being in the proximity of the surface. With the standard parameters and no arbitrary cutoff limits, five fields associated to five physicochemical properties, namely steric (S), electrostatic (E) and hydrophobic effects (H) and hydrogen bond donor (D) and acceptor (A) indices were calculated. The steric contribution was reflected by the third power of the atomic radii of the atoms. The electrostatic descriptors are derived from atomic

partial charges, and the hydrophobic fields are derived from atom-based parameters developed by Viswanadhan, and the hydrogen bond donor and acceptor indices are obtained by a rule-based method derived from experimental values [18].

PLS Analysis

Partial least squares statistical method [19] used in deriving the 3D-QSAR models is an extension of multiple regression analysis in which the original variables are replaced by a small set of their linear combinations. PLS method with leave-one-out (LOO) cross-validation was used in this study to determine the optimal numbers of components using cross-validated coefficient Q^2. The external validation of various models was performed using a

test set of five molecules. The final analysis (non-cross-validated analysis) was carried out using the optimum number of components obtained from the cross-validation analysis to get correlation coefficient (R^2). The Q^2 value determines the internal predictive ability of the model while R^2 value evaluates the internal consistency of the model [20]. Thus, the best QSAR model was chosen based on a combination of Q^2 and R^2.

Y-Randomization Test

The obtained models were further validated by the Y-Randomization method [21]. The Y vector (-logMIC) was randomly shuffled many times and after every iteration which led to a new QSAR model. The new QSAR models are expected to have lower Q^2 and R^2 values than those of the original models. This technique was carried out to eliminate the possibility of the chance correlation. If higher values of the Q^2 and R^2 are obtained, it means that an acceptable 3D-QSAR model cannot be generated for this dataset because of the structural redundancy and chance correlation.

Molecular Docking

The Surflex-Dock [8] was applied to study molecular docking by using an empirical scoring function and a patented search engine to dock ligands into a protein binding site. Mycobacterium tuberculosis receptor was retrieved from the RCSB Protein Data Bank (PDB entry code: 5UH5) [22]. The ligands were docked into corresponding protein binding site using an empirical scoring function and a patented search engine in Surflex-Dock. All water molecules in 5UH5 were deleted and the polar hydrogen atoms were added. Protomol, a computational representation of a ligand making every potential interaction with the binding site, was applied to guide molecular docking and predicted binding mode. All protomols could be established by three ways: (1) automatic: Surflex-Dock finds the largest cavity in the receptor protein; (2) ligand-based: a ligand in the same coordinate space as the receptor; (3) residues-based: specified residues in the receptor [23,24]. The R value is used to inspect the quality of the PDB file. R is a measure of error between the observed intensities from the diffraction pattern and the predicted intensities calculated from the

model. R values of 0.20 or less are taken as evidence that the model is reliable [25]. The R value of 5UH5 was 0.194 which revealed the quality of this PDB file [22].

In this study, we applied automatic docking: the 5UH5 structure was utilized in the subsequent docking experiments without energy minimization with other parameters established by default in the software. Surflex-Dock scores (total scores) were expressed in -log10(K_d) units to represent binding affinities. Then, the MOLCAD (Molecular Computer Aided Design) program was employed to visualize the binding mode between the protein and ligand. MOLCAD calculates and exhibits the surfaces of channels and cavities, as well as the separating surface between protein subunits [26-28]. MOLCAD program provides several capabilities to create a molecular surface. The fast Connolly method using a marching cube algorithm to engender the surface was applied in this work, thus the MOLCAD Robbin and Multi-Channel surface program exhibited with copious potentials were used. Moreover, Surflex-Dock total scores, representing binding affinities, were applied to estimate the ligand-receptor interactions of newly designed molecules. Every optimized conformation of each molecule in the data set was energetically minimized employing the Tripos force field and the Powell conjugated gradient algorithm with a convergence criterion of 0.05 kcal mol^{-1} A˚ and Gasteiger-Huckel charges [17].

In Silico ADME&T Properties

ADME&T (Absorption, Distribution, Metabolism, Excretion and Toxicity) processes are nowadays routinely carried out at an early stage of drug discovery to reduce the attrition rate [29]. In order to help minimizing failures, computational strategies are still sought by biopharmaceutical researchers to predict the fate of drugs in the organism, and to identify early the risk of toxicity. For this purpose, ADME&T related in silico models are commonly used to provide a fast and preliminary screening of ADME&T properties before compounds are further investigated *in vitro*. Both private industries and academic researchers have extensively studied properties related to ADME&T, including the inhibition of the transporter P-glycoprotein (ABCB1 or Pgp) or enzymes of the cytochrome P450 (CYP) family, in addition to the membrane permeability, volume of distribution and renal

Table 2. PLS Statistics of CoMFA and CoMSIA Models

Model	Q^2	R^2	S_{cv}	F	N	r_{ext}^2	Fractions				
							Ster	Elec	Acc	Don	Hyd
CoMFA	0.63	0.85	0.19	18.9	2	0,77	0.650	0.350	-	-	-
CoMSIA	0.65	0,71	0.173	26.68	2	0,65	0.040	0.054	0.384	0.00	0.522

Q^2) Cross-validated correlation coefficient. R^2) Non-cross-validated correlation coefficient. r_{ext}^2) External validation correlation coefficient. S_{cv}) Standard error of the estimate. F) F-test value Optimum number of the components.

clearance [30,31].

RESULTS AND DISCUSSION

CoMFA Results

Results of Table 2 demonstrate that CoMFA model has high R^2 (0.85) and F (18.90) values, and a small S_{cv} (0.19) as well as cross-validated correlation coefficient Q^2 (0.63) with two as optimum number of components. The external predictive capability of a QSAR model is generally cross checked and validated using test sets. The five randomly selected test sets-were optimized and aligned in the same manner as training sets. The external validation gave high value of r_{ext}^2 (0.77) indicating that prediction ability of CoMFA model is acceptable. The ration of steric to electrostatic contributions were found to be 65:35 indicating that-steric interactions are much more important than electrostatic.

CoMSIA Results

Different combinations between hydrophobic, electrostatic, steric, donor and acceptor fields were generated to explain the effects of substituents on anti-tuberculosis activity. The best CoMISA proposed model contains four fields, while hydrophobic and acceptor hydrogen contours describe more than 90% of CoMSIA results.

The standard error was 0.173 and the optimal number of principal components used to generate the CoMSIA model was two. The cross-validated correlation coefficient Q^2 value of the training set and non-cross-validated correlation coefficient R^2 gave 0.65 and 0.71, respectively. External

validation was used to confirm the ability of the proposed model, r_{ext}^2 value obtained was 0.65 which indicated the good stability of the predictive CoMSIA model.

Interpretation of CoMFA and CoMSIA Results

CoMFA and CoMSIA contour maps were generated to rationalize regions where the activity can be increased or decreased. The CoMFA and CoMSIA contour maps are shown in Figs. 3 and 4, respectively. Compound 13 was used as a reference structure.
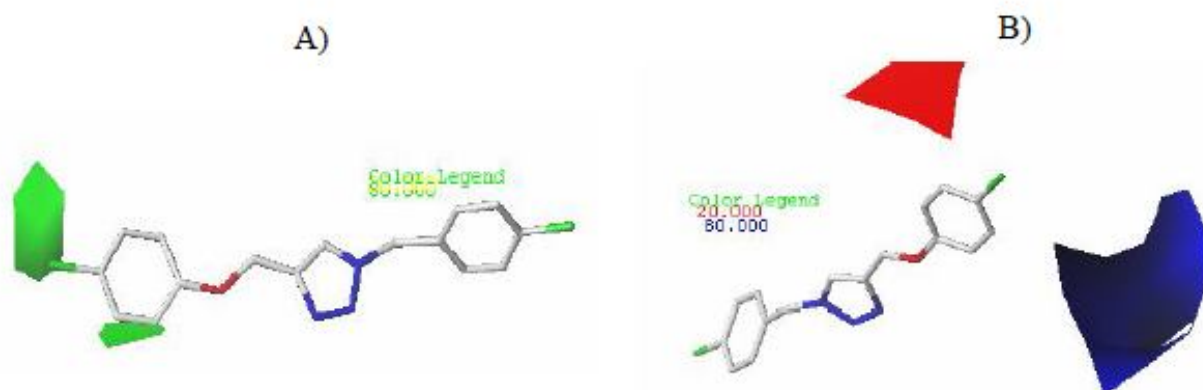
CoMFA Contour Maps

CoMFA electrostatic interactions are presented with red and blue colors while steric interactions are presented with green and yellow colored contours. The bulky substituents are favored around green regions, while yellow regions bulky groups are unfavored.

Nucleophile groups can increase the activity around red contours; and blue regions indicate that positive charges are favored.

The green and blue contours around R6 and R3 positions in the Fig. 3 that indicate electro-positive bulky groups are favored and could increase the activity. The red contour around R2 position indicates that electron donating groups can increase the activity.

CoMSIA Contour Map

According to CoMSIA fractions presented in Table 2, H-bond acceptor fields and Hydrophobic fields (0.384 and 0.522) are the major fields which can describe the activity, while steric and electrostatic fields (0.040 and 0.054) have no influence on the activity. The contour maps presented in

Fig. 3. Std* coeff. contour maps of CoMFA analysis with 2 Å grid spacing in combination with compound 13. A) Steric fields: green contours (80% contribution) indicate regions where bulky groups increase activity, while yellow contours (20% contribution) indicate regions where bulky groups decrease activity. B). Electrostatic fields: blue contours (80% contribution) indicate regions where groups with electropositive character increase activity, while red contours (20% contribution) indicate regions where groups with negative charges increase activity.
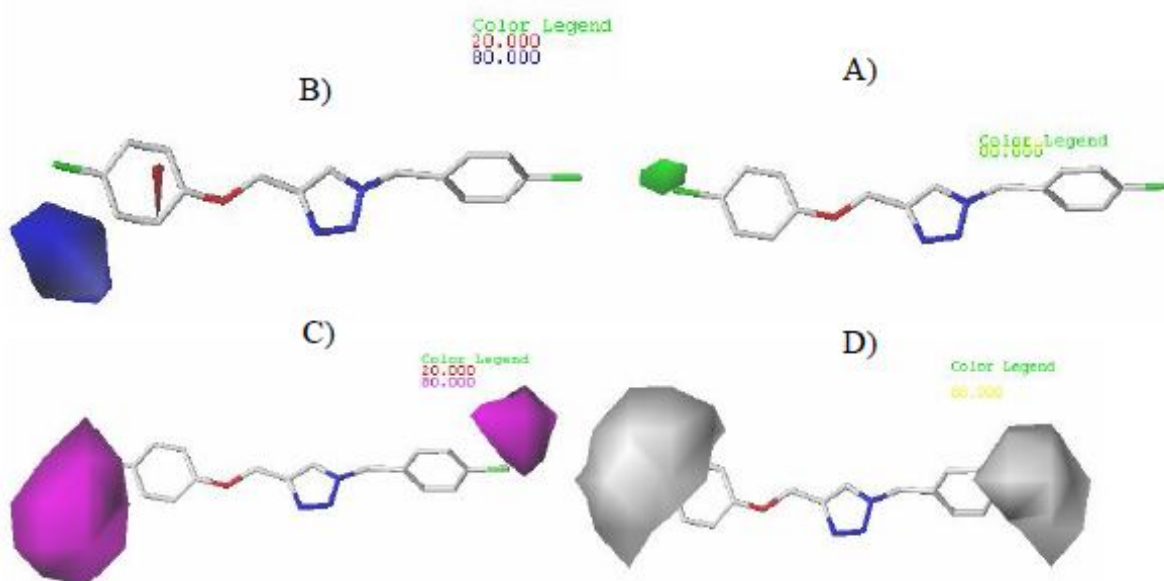
Fig. 4. Std* coeff. contour maps of CoMSIA analysis with 2 Å grid spacing for compound 13. A) Steric fields: green contours (80% contribution) indicate regions where bulky groups increase activity, while yellow contours (20% contribution) indicate regions where bulky groups decrease activity. B) Electrostatic fields: blue contours (80% contribution) indicate regions where electropositive groups increase activity, while red contours (20% contribution) indicate regions where electronegative groups increase activity. C) H-bond acceptor fields: The purple (80% contribution) and red (20% contribution) contours favorable and unfavorable positions for hydrogen bond acceptors respectively. D) Hydrophobic fields: yellow contours (80% contribution) indicate regions where hydrophobic properties were favored, while white contours (20% contribution) indicate regions hydrophilic properties were favored.

Fig. 4 indicate that hydrophilic groups with H-bond acceptor character increase the activity.

These contour maps explain why compounds 15, 13, 23 with H-bond acceptor groups and hydrophilic character in R_3 and R_6 positions ($R_3 = R_2 = Cl$) have good activities, also bulky groups in R_4 position ($R_4 = CH_3$) present good anti-tubercular activity, while compounds 16 and 20 with electronegative groups in R_2 ($R_2 = NO_2$) shows low activity.

Y-Randomization

To validate CoMFA and CoMSIA models different random shuffles of dependent variable were executed, and 3D-QSAR model was developed for each shuffle. The obtained results presented in Table 3 indicate that the original CoMFA and CoMSIA models are not due to a chance correlation of the training set.

Design for New Molecules with Anti-tubercular Activity

Relying on CoMFA and CoMSIA models, new molecules were designed to enhance the activity, as indicated in Table 4. These compounds were aligned to database using compound 13 as a template. The newly predicted structure A1 showed higher activity (pMIC = 5.8 and 5.83 for CoMFA and CoMSIA models, respectively) than compound 15 (the most active compound of database).

Table 4. Chemical structure of the newly designed molecules and their predicted pMIC based on CoMFA and CoMSIA 3D-QSAR models

To examine the stability of these new drugs and the interactions of these predicted molecules with the receptor, we used surflex-docking.

Docking Results

Molecular docking protocols are widely using to investigate the binding modes between the ligand derivatives and the receptor which help understanding the 3D-QSAR study revealed by CoMFA/CoMSIA models. The target ligand taken from the crystal structure is redocked into the active site to validate the accuracy of molecular docking, the root mean square deviation (RMSD) value is 1,12 Å. Figure 5 shows the different top 10 positions of molecule 15 in the tuberculosis protein pocket which present a stable conformation compared to compound 16

with scoring 3.06 and 1.71, respectively.

Subsequently, the active compound 15, inactive comound16, and the proposed compound A1 were docked into the ligand-binding pocket of tuberculosis protein (code PDB: 5UH5), as described in Figure 6. Docking results of the low active compound shows carbon-hydrogen bond with TYR F: 346 and THR F: 345 residues, pi-alkyl interaction with LYS F: 339 residue and van der Waals bond with ASP F: 336. Also the presence of unfavorable bond with TRP F: 349 can explain the low activity of compound 16. While compound 15 shows pi-alkyl and pi-pi interactions with TYR F: 341; PHE F: 335 and LYS F: 339 residues, beside van der Waals interaction with THR F: 345 with absence of unfavorable interactions. These results can explain the stability of compound 15 in the receptor pocket compared to compound 16.

Based on CoMFA/CoMSIA contour maps, the hydrophilicity of bulky compounds with electropositive character in R_3 and R6 positions could increase the activity. This prediction is confirmed by the results presented in Fig. 6. The proposed compounds present van der Waals interactions with LYS F: 342, ASP F: 336, PHE F: 335, THR F: 345 residues, pi-Alkyl and pi-pi bonds with LYS F: 339 and TYRF: 341 residues, pi-ion pair interaction with TRP F: 349 residue, also pi-donor hydrogen interactions with TYR F: 346 and LYS F: 334 residues. These receptor-ligand interactions explain the stability and the high activity of the proposed compound A_1. Moreover, the results obtained by docking were compared with the QSAR results to be verified mutually, it matches well with the results of H-bond acceptor/electrostatic contour maps obtained in CoMSIA contours.

Drug-likeness or Druggability

Depending on lipinski's rule, lead compounds with more than 5 hydrogen-bond donors, 10 hydrogen-bond acceptors, molecular weight (MW) over than 500 Da and logP more than 5, are known as poor absorption drugs [32]. Moreover, compounds with rotatable bonds ≤ 10 and total polar surface area ≤ 140 Å present good bioavailability [33].

In silico evaluation results of the proposed anti-tuberculosis drugs are in agreement with lipinski's rule of five and indicate a good oral bioavailability exceptionally compound A2 which present logP superior than 5.

Table 3. r^2 and Q^2 Values after Several Y-randomization Tests

Iteration	CoMFA		CoMSIA	
	Q^2	r^2	Q^2	r^2
1	0.13	0.07	-0.21	0.19
2	-0.04	0.52	0.17	0.32
3	0.22	0.16	0.08	0.56
4	-0.43	0.12	-0.14	0.26
5	-0.33	0.04	-0.5	0.22

Table 4. Chemical Structure of the Newly Designed Molecules and their Predicted pMIC Based on CoMFA and CoMSIA 3D-QSAR Models

No.	Structure						Predicted pMIC	
	R_1	R_2	R3	R4	R5	R6	CoMFA	CoMSIA
A1	$CH(C_2H_5)$	H	$HC(NO_2)Me$	H	H	Br	5.8	5.83
A2	$CH(C_2H_5)$	H	COCl	H	H	Br	5.4	5.26
A3	C_2H_5	H	$COCH_3$	H	H	NO_2	4.95	5.47
A4	C_2H_5	H	CH_3	H	H	NO_2	4.89	5.18
A5	H	H	$HC(NO_2)Me$	H	H	Br	5.24	5.03
A6	H	H	COCl	H	H	Br	4.98	4.87
A7	H	H	$COCH_3$	H	H	Br	5.12	4.88
A8	H	H	CH_3	H	H	Br	4.77	4.92
A9	H	H	$HC(NO_2)Me$	H	H	NO_2	4.81	4.96
A10	H	H	COCl	H	H	NO_2	4.77	4.72
A11	H	H	$COCH_3$	H	H	NO_2	4.87	4.75
A12	H	H	CH_3	H	H	NO_2	4.74	4.71

Moreover, TPSA, total hydrogen and rotatable bonds are within the limited ranges. Compounds with MW less than 500 Da are easily absorbed and diffused compared to heavy molecules [34]. These properties confirm the good bioavailability of the proposed anti-tuberculosis drugs.

ADMET Properties

During drug development process many drugs are failed
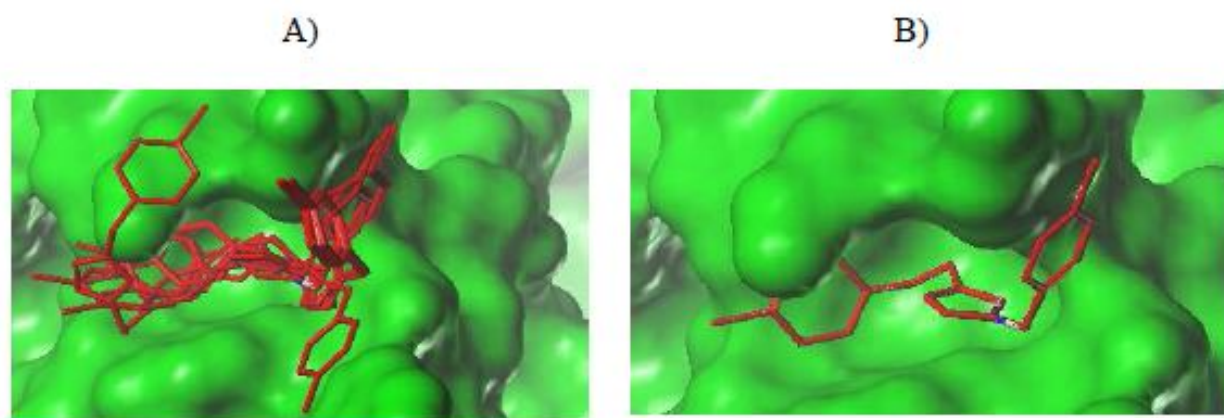
Fig. 5. La surface de MOLCAD du site allostérique dans le composé 15. A) Les dix différentes positions du composé 15 dans le récepteur. B) la position stable du composé 15 dans le récepteur.

Table 5. Physicochemical Parameters of the Four Lead Compounds

	logP	MW	TPSA	HBD	HBA	nrotb
Compound A1	4.64	487.35	85.76	0	7	9
Compound A2	5.17	448.74	57.01	0	5	7
Compound A3	3.10	380.40	102.80	0	7	8
Compound A4	3.21	354.41	85.76	0	6	7

due to blood brain permeation problems, toxicity and poor absorption. The aim of preclinical ADMET study is to eliminate weak candidates and focus on succeeded drug candidates.

This review treats the applicability of the proposed compounds as anti-tuberculosis agents using virtual properties, absorption, distribution, metabolism, excretion, and toxicity (ADMET) which are key players in drug development.

The pharmacokinetic (ADMET) properties of the studied leads were calculated using pKCSM and admetSAR predictor. Blood-brain barrier (BBB) penetration, human intestinal absorption (HIA), Caco-2 cell permeability, and AMES test are used to refine the drug likeness properties. The main interfaces separating the central nervous system (CNS) and the blood circulation are known as the blood-brain barrier (BBB) which is an important property since it

determines if drugs can pass the blood-brain barrier or not, and also exerts its effect on the brain [35]. Compound with logBB < -1 is considered poorly distributs to the brain. The BBB permeability results in Table 6 show non-penetrating BBB for new anti-tuberculosis compounds.

Molecule with an absorbance less than 30% is considered to be poorly absorbed, indicating that all tested compounds could be absorbed by the human intestine, however, the two proposed compounds A1 cannot penetrate to Caco-2 (high permeability would translate in predicted value superior than 0.9). Nevertheless, the tested compound A1 proved to be potential substrate for P-glycoprotein (P-gp) which effluxes drugs and various compounds to undergo further metabolism and clearance [36].

The inhibition of cytochrome P450 isoforms might cause drug-drug interactions in which co administered drugs fail to be metabolized and accumulate to toxic levels [37].
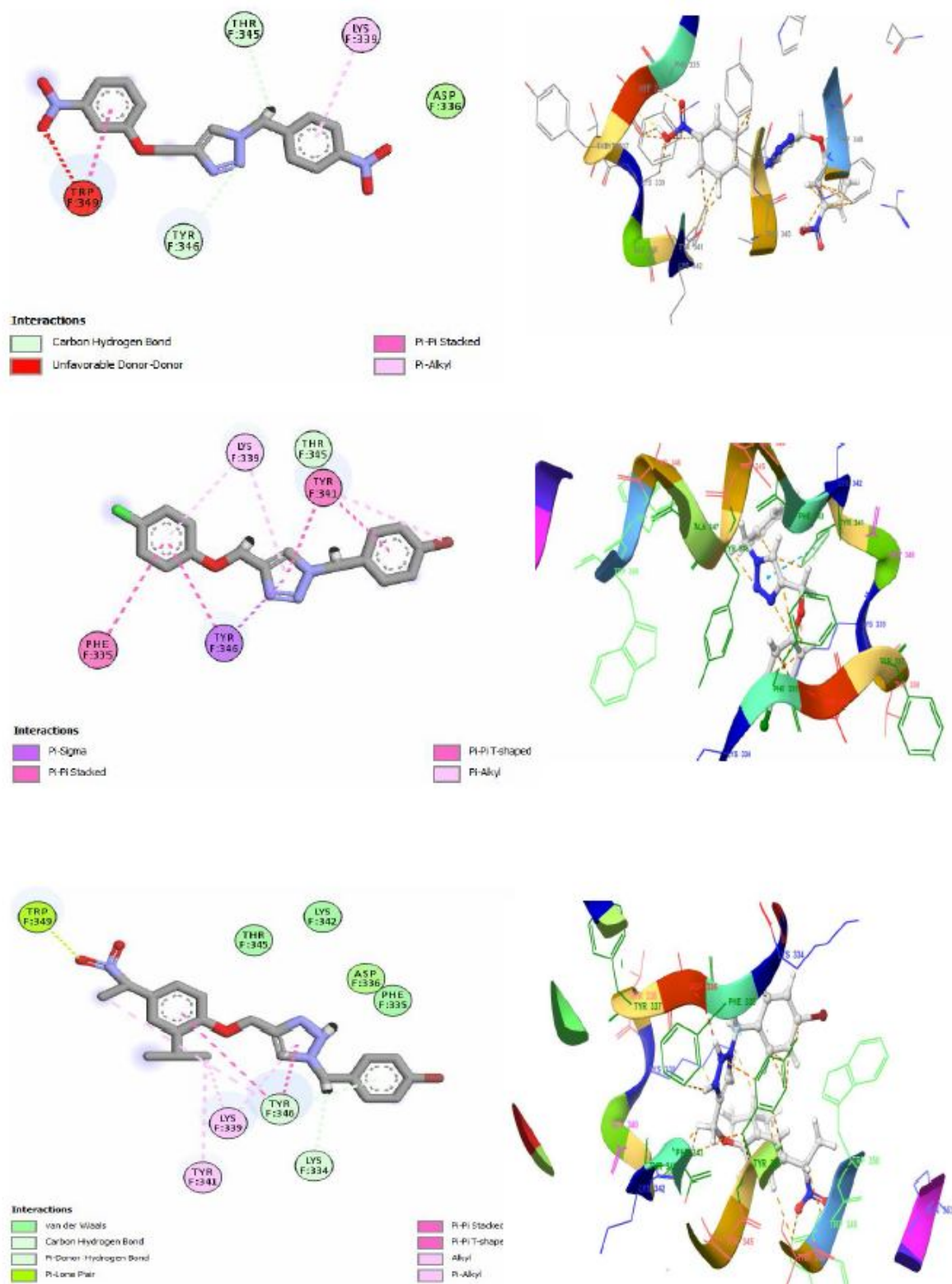
Fig. 6. Docking interactions of compounds 16, 15 and the proposed compound A1.

Table 6. Pharmacokinetic (ADMET) Properties of the New Anti-tuberculosis Agents

Models	Compound A1	Compound A2	Compound A3	Compound A4
Absorption and distribution				
Blood-brain barrier (logBB)	-1.277	-0.343	-1.064	-0.477
Intestinal absorption (human)	96.47	94.74	100	89.53
Caco-2 permeability	0.558	1.058	1.044	0.917
P-glycoprotein substrate	Substrate	Non-substrate	Non-substrate	Non-substrate
P-glycoprotein inhibitor	Non-inhibitor	Inhibitor	Inhibitor	Inhibitor
metabolism				
CYP2D6 substrate	No	No	No	No
CYP450 3A4 substrate	Yes	Yes	Yes	Yes
CYP1A2 inhibitor	No	Yes	Yes	Yes
CYP 2C9 inhibitor	Yes	Yes	Yes	Yes
CYP2D6 inhibitor	No	No	No	No
CYP2C19 inhibitor	Yes	Yes	Yes	Yes
CYP3A4 inhibitor	Yes	Yes	No	Yes
Excretion and toxicity				
Clearence	-0.013	-0.195	0.248	0.415
AMES toxicity	No	Yes	Yes	Yes
Carcinogens	Non-carcinogens	Non-carcinogens	Non-carcinogens	Non-carcinogens

Notwithstanding, some of the cytochrome P450 isoforms could be inhibited by one or more of the proposed compounds. Fortunately, our best candidate compound A1 did not show any acute toxicity and mutagenic effect with respect to the Ames test data.

CONCLUSIONS

Several 1,2,3-triazole analogues were identified as potentially effective oral anti-tubercular agents through a series containing 31 compounds of computer-aided drug design processes, such as 3D-QSAR modeling and molecular docking. CoMFA/CoMSIA models showed good internal and external validation abilities with interesting statistical capacity. Based on their contour maps new potent molecules were developed which showed high anti-tubercular activity. Meanwhile, molecular docking process was established to study the possible binding modes with

Mycobacterium tuberculosis (MTB) receptor at the active pocket, and to identify the nature of interactions between ligands and residues. In addition, in silico ADMET study showed good properties for the new proposed compound A1 which could be the great ligand targeting tuberculosis. Overall, these results indicate that the optimal CoMFA/ CoMSIA models, molecular docking and ADMET properties can be used to predict novel anti-tubercular agents and guide the discovery of new potential analogues.

ACKNOWLEDGMENTS

We are grateful to the "Association Marocaine des Chimistes Théoriciens" (AMCT) for its pertinent help concerning the programs.

Conflict of Interest
There's no conflict of interest.

Statement of Human and Animal Rights
This article does not contain any studies with human or animal subjects performed by any of the authors.

REFERENCE

[1] R.G. Ducati, A. Ruffino-Netto, L.A. Basso, D.S. Santos 101 (2006) 697.

[2] R.C. Brito, C. Gounder, D.B. De, Lima, H. Siqueira, H.R. Cavalcanti, M.M. Pereira, A.L. Kritski, JBP. J. Brasileiro de Pneumologia 30 (2004) 425.

[3] K. Roy, S. Kar, R.N. Das, A Primer on QSAR/QSPR Modeling, 2015.

[4] H.G. Jeong, Y.W. Lee, Cancer Lett. 134 (1998) 73.

[5] R.D. Cramer, D.E. Patterson, J.D. Bunce, JACS 110 (1988) 5959.

[6] G. Klebe, U. Abraham, T. Mietzner, J. Med. Chem. 37 (1994) 4130.

[7] M.H. Shaikh, D.D. Subhedar, L. Nawale, D. Sarkar, F.A. Kalam Khan, J.N. Sangshetti, B.B. Shingate, Med. Chem. Commun. 6 (2015) 1104.

[8] M.O. St. Louis, SYBYL-X, version 2.0. Tripos Associates, USA, 2012.

[9] Discovery Studio Visualizer, Accelrys Software, 2016.

[10] D. Cao, J. Wang, R. Zhou, Y. Li, H. Yu, T. Hou, JCIM 52 (2012) 1132.

[11] D.E.V. Pires, T.L. Blundell, D.B. Ascher, J. Med. Chem. 58 (2015) 4066.

[12] M. Clark, R.D. Cramer, N. Van Opdenbosch, J. Comp. Chem. 10 (1989) 982.

[13] W.P. Purcell, J.A. Singer, J. Chem. Eng. Data 12 (1967) 235.

[14] M.D.M. Abdulhameed, A. Hamza, J. Liu, C.G. Zhan, J. Chem. Inf. Model 48 (2008) 1760.

[15] A. Aouidate, A. Ghaleb, M. Ghamali, *et al.* J. Struct. Chem. 29 (2018) 1031.

[16] L. Ståhle, S. Wold, Prog. Med. Chem. 25 (1988) 291.

[17] B.L. Bush, R.B. Nachbar, J. Comput. Aided Mol. Des. 7 (1993) 587.

[18] V.N. Viswanadhan, A.K. Ghose, G.R. Revankar, R.K. Robins, J. Chem. Inf. Comp. Sci. 29 (1989) 163.

[19] S. Wold, Quant, Struct. Act. Relat. 10 (1991) 191.

[20] M. Baroni, S. Clementi, G. Cruciani, G. Costantino, D. Riganelli, E. Oberrauch, J. Chemo. 6 (1992) 347.

[21] C. Rücker, G. Rücker, M. Meringer, J. Chem. Inf. Model. 47 (2007) 2345.

[22] W. Lin, K. Das, Y. Feng, R.H. Ebright, Mol. Cell. 66 (2017) 169.

[23] A.N. Jain, J. Med. Chem. 46 (2003) 499.

[24] J. Sun, S. Cai, H. Mei, J. Li, N. Yan, Y. Wang, J. Mol. Mod. 16 (2010) 1809.

[25] S. Gharaghani, T. Khayamian, M. Ebrahimi, SAR QSAR Environ. Res. 24 (2013) 773.

[26] Y. Ai, S.-T. Wang, P.-H. Sun, F.-J. Song, Inter. J. Mol. Sci. 11 (2010) 3705.

[27] P. Lan, W.N. Chen, W.M. Chen, Eur. J. Med. Chem. 46 (2011) 77.

[28] P. Lan, W.N. Chen, G.K. Xiao, P.H. Sun, W.M. Chen, Bioorg. Med. Chem. Lett. 20 (2010) 6764.

[29] G. Caldwell, Z. Yan, W. Tang, M. Dasgupta, B. Hasting, Curr. Top. Med. Chem. 9 (2009) 965.

[30] H.E. Selick, A.P. Beresford, M.H. Tarbit, Drug Discov. Today 7 (2002) 109.

[31] R. Gujjar, F. El Mazouni, K.L. White, J. White, S. Creason, D.M. Shackleford, P.K. Rathod, J. Med. Chem. 54 (2011) 3935.

[32] C.A. Lipinski, F. Lombardo, B.W. Dominy, P.J.

Feeney, Adv. Drug Deliv. Rev. 46 (2001) 3.

[33] D.F. Veber, S.R. Johnson, H.Y. Cheng, B.R. Smith, K.W. Ward, K.D. Kopple. J. Med. Chem. 45 (2002) 2615.

[34] V. Srimai, M. Ramesh, K.S. Parameshwar, T. Parthasarathy, Med. Chem. Res. 22 (2013) 5314.

[35] R.K. Upadhyay, Bio. Med. Res. Inter. 2014 (2014) 37.

[36] M.L. Amin, Drug Target Insights 2013 (2013) 27.

[37] T. Lynch, A. Price, American Family Physician 76 (2007) 391.